Fabrication of TiO_2 Based Dye-Sensitized Solar Cell with Natural Dyes

M.Sc. Thesis

By

Rahul Lamba

DISCIPLINE OF PHYSICS

INDIAN INSTITUTE OF TECHNOLOGY INDORE

JUNE, 2019

Fabrication of TiO_2 Based Dye-Sensitized Solar Cell with Natural Dyes

A THESIS

Submitted in partial fulfillment of the requirements for the award of the degree

of

Master of Science

by

Rahul Lamba

DISCIPLINE OF PHYSICS

INDIAN INSTITUTE OF TECHNOLOGY INDORE

JUNE, 2019

INDIAN INSTITUTE OF TECHNOLOGY INDORE

CANDIDATE'S DECLARATION

I hereby certify that the work which is being presented in the thesis entitled **Fabrication of TiO_2 Based Dye-Sensitized Solar Cell with Natural Dyes** in the partial fulfillment of the requirements for the award of the degree of **MASTER OF SCIENCE** and submitted in the **DISCIPLINE OF PHYICS, Indian Institute of Technology Indore**, is an authentic record of my own work carried out during the time period from July 2017 to June 2019 under the supervision of Dr. Parasharam M. Shirage, Associate Professor. The matter presented in this thesis has not been submitted by me for the award of any other degree of this or any other institute.

Rahul Lamba

Signature of the student
RAHUL

This is to certify that the above statement made by the candidate is correct to the best of my/our knowledge.

28/6/2019

Signature of the Supervisor

DR. PARASHARAM M. SHIRAGE

RAHUL has successfully given his M.Sc. Oral Examination held on **20 June 2109.**

28/6/2019

Signature of Supervisor
Dr. Parasharam M. Shirage
Date:

Convener, DPGC
Date: 1/7/19

Signature of PSPC Member
Dr. Preeti Bhobe
Date: 1/7/19

Signature of PSPC Member
Dr. Hemant Borkar
Date: 01/07/19

ACKNOWLEDGEMENTS

Firstly, I would like to express my sincere gratitude to my thesis advisior **Dr. Parasharam M. Shirage** for the continuous support in my M.Sc. project and related research, for his patience, motivation, and immense knowledge.

I would like to thank and express solicit gratitude to our director **Professor Pradeep Mathur** for proving all facility and giving me opportunity to work in a nice environment.

I would take the opportunity to express my gratitude to my PSPC members **Dr. Preeti Bhobe** and Dr. Hemant Borkar for their valuable suggestions.

I am particularly grateful for the assistance given by **Mr. Vishesh Manjunath** for his valuable and constructive suggestions during the planning and development of this research work. I would like to express my very great appreciation to **Suchi Agrawal** for her willingness to give her time so generously and helping me at everything.

I would also like to extend my thanks to all AFMRG lab members. I am grateful to all members of AFMRG lab for constant motivation and entertaining discussions. Special note of thanks **to Ms. Lichchhavi Sinha, Ravi, Kalpana, Neetu, Priyanka, Manoj Kumar, Rahul Yadav, Vivek Chauhan, Nikhil Kumar Shubham** for their support and love throughout project work. Am thankful to HoD and DPGC Physics for constant support.

Finally, I must express my very profound gratitude to my parents for providing me with unfailing support and continuous encouragement throughout my years of study and through the process of researching and writing this thesis.

Abstract

A dye-sensitized solar cell (DSSC) belongs to thin film solar cells, based on a semiconductor formed between photoelectrode, electrolyte, and counter electrode which utilizes the benefit of the wide band gap semiconductor with dye absorbed on it, that sensitized to the light. At the heart of the device, a thick oriented nanorod film of titanium dioxide (TiO_2) is present as wide bandgap semiconductor. The idea of the dye in DSSC is same as chlorophyll in leaves; as it absorbs a photon, dye molecules get excited and injects electron to a wide bandgap semiconductor(here TiO_2) to generate electricity. DSSCs are assembled using abundant and inexpensive materials by economical methods.

The work carried during this project aimed on optimizing the DSSC using two different strategies; by synthesizing TiO_2 nanostructures for DSSCs photoelectrode and by checking the nature of dyes for DSSCs application. We used different natural dyes extracted from various plants, flowers, fruits, and measured their I-V characteristics.

The best optical and photovoltaic performance in terms of efficiency and stability achieved with polypyridyl complexes of ruthenium and osmium, which are commercial dyes, but here natural dyeshas been used to construct Gratzel cells.

TABLE OF CONTENTS

LIST OF FIGURES

ACRONYMS

DSSC	Dye-Sensitized Solar Cell
FTO	Fluorine doped Tin Oxide
ITO	Indium doped Tin Oxide
TCO	Transparent conductive glass
TiO_2	Titanium dioxide
PV	Photovoltaic
FESEM	Field Emission Scanning Electron Microscope
XRD	X-Ray Diffraction
ZnO	Zinc Oxide
1 D	One dimensional
AM	Air Mass
CdTe	Cadmium telluride
HOMO	Highest occupied molecular orbit
LUMO	Lowest unoccupied molecular orbit
CB	Counduction band
KI	Potassium Iodide
DI	Deionised Water

Chapter 1

Introduction

"If we knew what it was we were doing, it would not be called research, would it?"

~Albert Einstein

We all depend on solar energy, and the Sun is the most opulent renewable energy source, which radiates energy in the form of solar radiation. Amount of energy from sunlight strikes the earth's surface in 1 hr is more than all the energy consumed by humans in an entire year, which is around 430 quintillion Joules of energy. It's 430 with eighteen zeros after it [1]. Now the question arises why we are talking about solar energy? So, we are currently using fossil fuels like oil, coal, and gas which are the nonrenewable source of energy and are in limited stock and produce a lot of pollution while it's uses. And as increasing demand[2], non renewable fuel resourses will vanish soon, but solar energy is a continuous and inexhaustible energy resource with no pollution.

Now, How to harness this solar energy?

Some technologies are available in the market like solar thermal technology, artificial photosynthesis, and photovoltaic cells. As we are working on the solar cell, it is the photovoltaic cell which converts sunlight directly to electricity, with no pollution, and with large handling capacity, it can be the future of the energy sector.In India, approximately 34% of the overall energy utilization is being provided by the renewable sources eg., solar, wind, biomass and etc,.

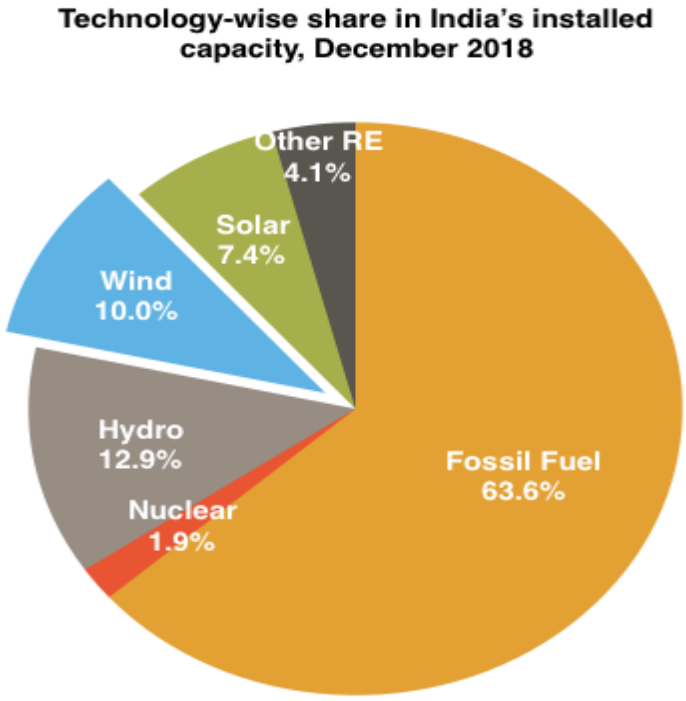

Figure.1 Energy share in india in December 2018 [3]

After fossil fuel largest share comes from hydrothermal which is 13% but hydrothermal is not a pivotal solution to fulfill energy demand in the near future. Wind energy is good, but it outperformed by photovoltics. Photovoltaics in terms of generating power is more advantageus and huge scope of improvement can be seen. Till 2030, photovoltaics for electricity generation will generates 50% of the overall energy [4]. In photovoltaic R&D trying to decrease manufacturing cost with an increase in efficiency by using cheap and non toxic material with a simple synthesis. A silicon-based solar cell is available in the market with efficiency around 19% [5], but it's manufacturing cost is very high, and during production, it produces non-environment friendly waste. The Dye-sensitized solar cell was first created by M.Gratzel in 1991. This further developed in 1992 by using TiO_2 nanostructure it is an alternative method for Si-based solar cell. It has an advantage of higher efficiency at low cost and good price/performance ratio [6]. It can work at low light and wider angles and

its mechanical robust. Highest efficiency for DSSC is achieved around 11% using Rubidium based commercial dyes[7]. So we fabricated DSSC using natural dyes in this project.

When analyzed on the basis of efficiency which based on conversion mechanism, in a standard p-n junction, the mechanism behind the production of electricity is by charge separation and conduction [8]. In Gratzel cells energy is absorbed by dye molecule and get excited, injecting electron to the conduction band of TiO_2 and its move through load doing work in the form of producing electric energy and come back to counter electrode and recombine using an electrolyte[9]. This process is already discussed in the reports reported earlier.

The foremost part for photogeneration is photoanode in DSSC. The photoanode is consist of wide bandgap semiconductor with dye anchored on it as shown in Figure 1.2.

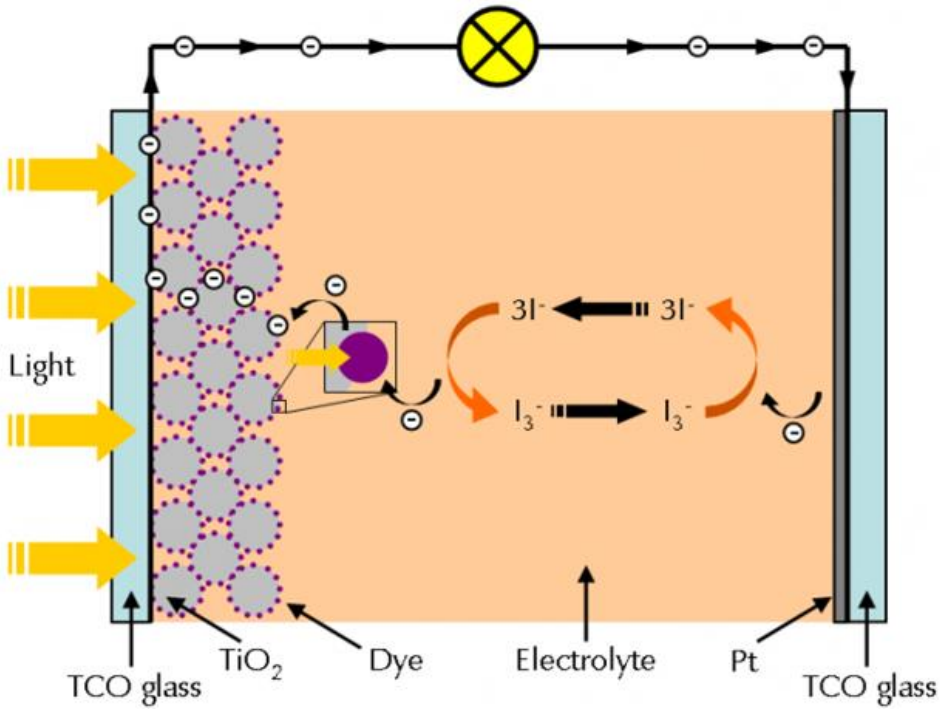

Figure 1.2 DSSC and its photoanode layers [1]

DSSC consists of TCO, a wide bandgap semiconductor, dye, electrolyte, and carbon coated TCO. FTO and ITO can be possibly TCO layers used;

here we use FTO as TCO due to its thermal stability during annealing at 450^0C [9]. To maximize interaction between FTO and wide bandgap semiconductor we grow TiO_2 nanorods on the FTO using hydrothermal reaction. We didn't use ZnO due it instability in acidic dye medium [10-11].

In this thesis, we have synthesized 1D nanorods of TiO_2 on FTO and extracted four dyes from different plants and fabricated the cell. The main motivation of doing this work is to reduce the cost by providing better efficiency by reengineering and designing each components of DSSC.

Chapter 2

Literature Survey

Earlier, we talked about how to harness solar energy by the fact of converting solar energy into electricity, bioenergy or heat. Here we will focus on Photovoltaic energy. Edmon Becquerel first discovered the photovoltaic effect in 1839 [12]. Later after half century, in 1883, the first solar cell panel was fabricated by Charles Fritts, a solar cell synthesis by the use of Se and Au, having efficiency 1%. In 1904, Albert Einstein discussed the mechanism pf photovoltaic, as the reason for the emission of electron is due to the absorption of photons, i.e,. packets of energy (quanta)[13] and after some research in solar cell, then comes DSSC in 1991 introduced by M.Gratzel and Brain O'Regan, developed in 1992 using TiO_2 nanostructure.

2.1. Solar radiance and Spectrum

Sun is reviewed as a blackbody at a temperature around 5800K, which radiates all kind of radiation according to Planck's law [14].

As photons show wave-like behavior, the relation between energy and wavelength given by Plank's law is

$$E=h\nu\lambda \qquad (2.1)$$

The solar energy gets absorbed by the various gases present in atmosphere or reflected back into space by the atmosphere hence the amount of energy we receive at earth surface is different for different location depends on the path traveled by sunlight and we define it by

$$Air\ Mass= 1/\cos\theta \qquad (2.2)$$

Where θ is the angle of incidence with zenith.

Solar radiation for extraterrial is AM 0, for $\theta = 0^0$ AM 1 and AM 1.5 when $\theta = 48.2^0$ which we use for solar radiation we receive at surface.

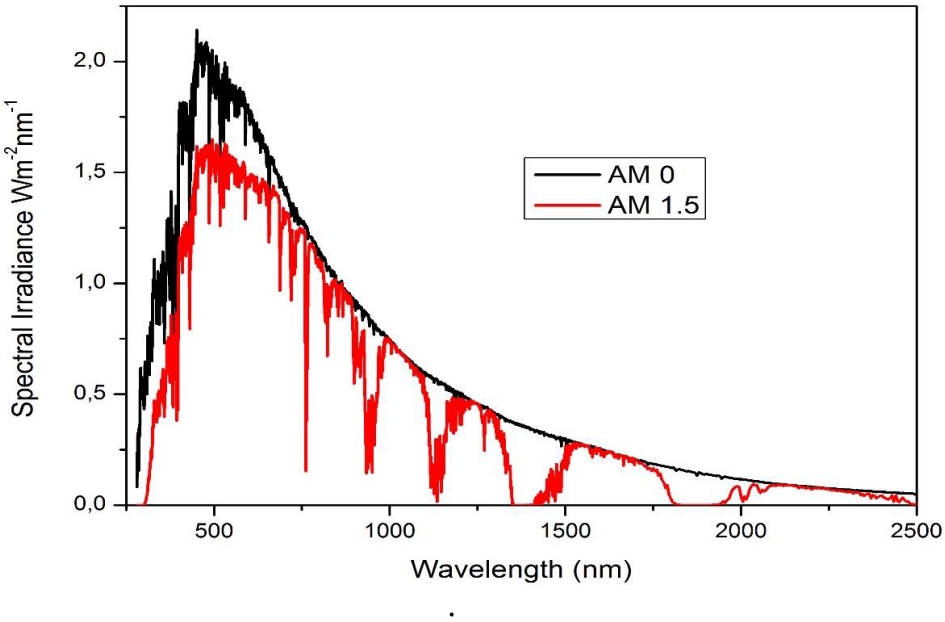

Fig. 2.1. Sun Solar Spectrum [15]

The area below the curve is given by Stefen-Boltzman law.

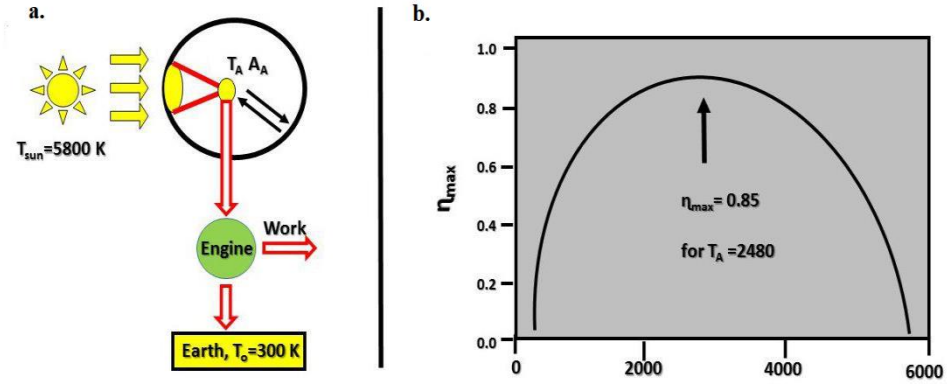

Figure 2.2 Simplified diagram of an solar cell arrangement (a), the theoretical conversion efficiency of solar radiation with temperature (b) [16].

2.2. Structure of Basic Solar Cell

A standard solar cell is built by two different doped semiconductor layers which are combined, and the junction formed is called p-n junction, by doping trivalent element in silicon, we get p-type semiconductor, and by doping pentavalent, we get n-type semiconductor. And by bringing them together, it forms a junction which has an inbuilt potential due to the flow of electron and hole.When it exposed to sunlight electron-hole pair forms, and due to inbuild potential, electrons flow through load doing work giving electricity. Electronic band gap of semiconductor must be low so the electron can get excites from valence band to conduction band at low ligh t [17] .

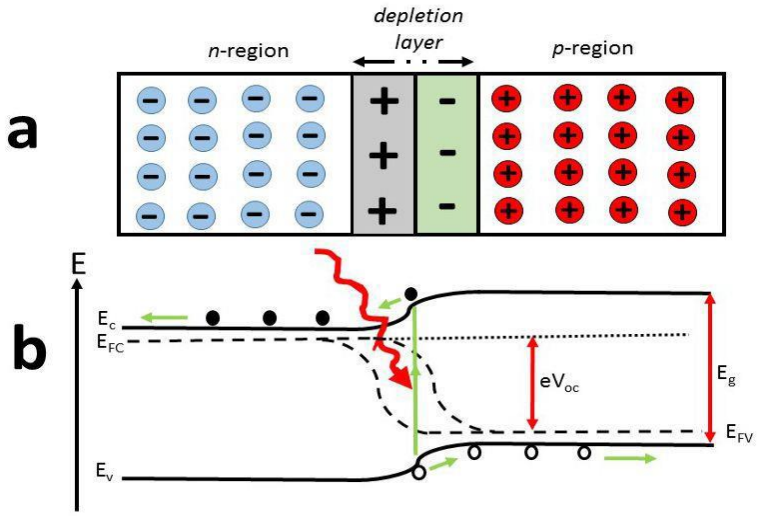

Figure 2.3 p-n semiconductor junction in equilibrium (a), diagram of energy band of a p-n junction under illumination (b) [16].

2.3. Brief Overview on Photovoltaic Technologies and Market

Solar cells are divided into three generations. In the first generation solar cell has basic crystalline silicon cells. Second generation solar cell consists of thin Film technologies and third generation we have organic, inorganic, hybrid, etc. solar cells and these technologies are not commercially available at a large scale.

The type of solar cell is discussed here with their efficiency and other details

Silicon solar cells

Silicon solar cells belongs to the first generation and widely commercially available with efficiency around

A) Monocrystalline silicon cells has an efficiency of around 24.7% .

B) Polycrystalline silicon cells have an efficiency of around 20.3%[18].

Problem with these is high manufacturing cost, and waste produced during manufacturing is not environment-friendly.

Thin film technologies

Thin film technology devices are amorphous Si(~13.4%), CdTe (~19%), CuInSe2 (~20.4%) and GaAs (~25.1%). Efficiency is good, but cells are not stable, and but we lowered the manufacturing cost. CdTe is the only rival of silicon cells, but cadmium is highly toxic. Due to the stability of these cell in not good, most of them are not available commercially. [18].

Organic and hybrid solar cells

DSSC comes in the second and third generation of a solar cell here we are using dye, which are organic and inorganic in nature. Highest Efficiency of DSSC is 12%.

Heterojunction Solar cell is a hybrid solar cell with an efficiency of 12%.

Perovskite solar cells

Perovskite Solar cell is of the third generation of the solar cell with good efficiency of 23.7%, but in the lead based perovskite, lead is toxic. And stability is a major issue in pervoskite solar cell [19].

2.4 The Shockley-Queisser limit

The Shockley-Queisser limit is referred to the calculation of maximum theoretical efficiency for solar cells constructed from a single p-n junction. It was first calculated by William Shockley and Hans Queisser in 1961 [20]. According to Shockley-Queisser limit maximum solar efficiency we can get from a p-n junction is around 33.7% with a band gap of 1.4 eV (AM 1.5), when incident radiation is one sun. Solar cell efficiency varies with semiconductor material bandgaps. The best silicon-based solar cell efficiency is reported at around 24%.

The Shockley-Queisser limit is applicable to all the solar cell.

2.5 Dye-Sensitized Solar Cell

Dye-sensitized solar cells belong to the third generation of solar, which is created by Micheal Gratzel and O'Regan[21].

As DSSC has a good price/ performance ratio and can work under a wider angle and low light,due to this interest in dye-sensitized solar cell increased recently [22].

Device Structure

As DSSC is consists of four main components Photo electrode & counter electrode, dye, electrolyte, and wide bandgap semiconductor.

Wide bandgap semiconductor is coated on TCO here we use TiO_2 nanorods as a semiconductor layer and FTO as transparent conducting oxide. We extracted four different-different dyes from various leaves, flower, and fruits, which are chlorophyll and anthocyanin-rich in nature. Further, we prepared our Iodide and triiodide electrolyte. On the counter electrode, we coated carbon layer by using a candle flame. DSSC is a sandwich type composition which can be seen in figure 2.4 The electrode with TiO_2 film on it, dye is absorbed using a dip coating method sandwiched with the counter electrode with electrolyte as an electron mediator in between wide bandgap semiconductor electrode and the counter electrode.

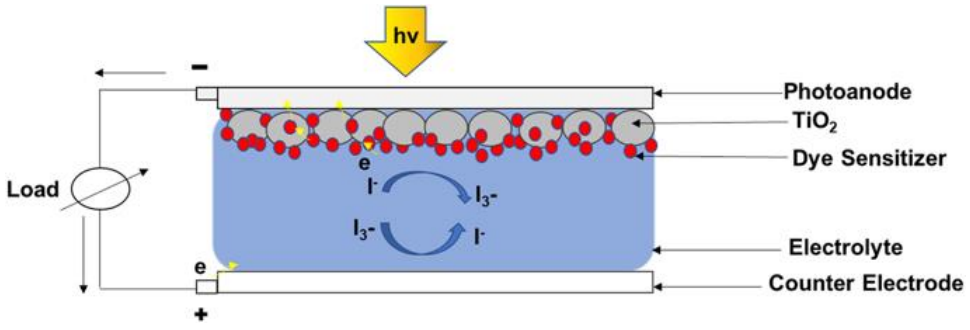

Figure 2.4 DSSC device structure [24]

Working

When a photon is absorbed by the dye molecule (S) it gets excited from HOMO to LOMO level [25]

$S + hv \longrightarrow S^*$

As the potential of the HOMO of the dye molecule is more than the semiconductor conduction band, the electron gets transfered to the conduction band of semiconductor where it flows freely.

$S^* \longrightarrow S^+ + e^-$ (CB)

The oxidized dye then regenerated by Iodide ion by receiving an electron from it.

$3I^- + 2S \longrightarrow I_3 + 2S$

$S^+ + e^- \longrightarrow S$

Iodide ion get Oxidized into Tri iodide ion further receives electron from the counter electrode and regenerate as iodide ion again.

$I_3 + 2e^- \longrightarrow 3I^-$

In this thesis, chlorophyll and anthocyanin-rich dyes were examined as a possible sensitizer for DSSC in contrast to other commercially available dyes. We fabricated DSSC cells with all four dyes and measured their IV characteristics and found out the efficiency As we were facing problems like the evaporation of liquid electrolyte and low injection rate of an electron from dye to nanostructured semiconductor [25], we have to optimize and re-engineer the DSSC components for better stability and efficiency.

2.6 Motivation for Work:

Currently, the solar cells which are available commercially based on inorganic silicon, the manufacturing cost is high, and during the production of this solar cell, it produces environmentally unfriendly waste. And as DSSC based on natural dyes which is very cheap to manufacture and a cost-efficient alternative for photovoltaic production.

As DSSC is a replica of the Photosynthesis process and here we are generating electricity from dye extracted from leaves of the plants, it always fascinates me, and this is the reason I'm working on DSSCs.

The utilization of the natural dyes will bring down the cost of the DSSC's hence they are promising to be researched.

The following objectives are proposed in the current research project.

2.7 Objectives:

- To synthesize TiO_2 nanostructures for DSSCs.
- To characterize synthesized materials, using XRD, SEM, UV- VIS and Raman spectroscopy for physical and chemical properties.
- To investigate photovoltaic response using dark and light I-V curve and estimate fill factor and efficiency.
- To check the nature of dyes for DSSCs application.
- To decide the future scope of the work.

Chapter 3

Synthesis and Experimental Technique

3.1 Sample preparation

Materials: Titanium(IV) Butoxide ($Ti(OBu)_4$), Manganese nitrate from Sigma-Aldrich, Deionized water, Ethanol (C_2H_5OH), Glacial Acetic acid, Nitric acid (HNO_3), Fluorine tin oxide (FTO) conducting glass slides, acetone (C_3H_6O), ethanol (C_2H_5OH) and were used without further purification.

3.1.1 Preparation of TiO_2 Nano rods:

Hydrothermal method

In this synthesis, We mix deionized water with undiluted hydrochloric acid to reach a final volume of 60 mL, and then the solution was stirred for five minutes using magnetic stirrer. Now we add Titanium butoxide into the mixer, and the mixture then again stirred for another five min. After stirring the mixture, it will look transparent. The mixer then transferred to an autoclave of capacity 100mL. Two or Three pieces of FTO substrates which ultrasonicated with acetone, 1-propanol, and methanol each for 15 minutes, then placed vertically conducting side facing the wall of the autoclave. The hydrothermal reaction was carried out at 100-200^{0}C for 10, 15, 20 hours. After synthesis, autoclave was brought down to 25^0 C by putting it at room temperature for some hours, and Then TCO substrate was taken out from autoclave, washed thoroughly with DI water and put it in open space to dry. When we used glass as a substrate and try to synthesize TiO_2 nanorods on it, all experiments failed.

3.1.2 Dye Synthesis

1. Red Grapes:

To derive the anthocyanin from the skin of grapes [26], first deionized water was used to washed grapes thoroughly, and then the skin from grapes was manually separated by hands. The skins obtained were dried in the furnace for 20 h at 40 °C, and then to extract anthocyanin at room temperature, we crushed dried skin by mortar pastel to a fine powder and then put for stirring in an ethanolic solution for overnight after that the extract was filtered. To get the concentrated extract, we use roto-evaporator at 60 °C. The anthocyanin rich ethanolic extract was stored in the dark, at a temperature below 5 °C.

2. Moss Rose:

The chlorophyll is collected from the leaves of Moss Rose plant leaves. The leaves were cleaned two or three times with deionized water to remove unwanted materials and then put it to dry at 60^0 C in a furnace for 20 h. The dry sample was then crushed using mortar and pastel and dissolved in ethanol. The mixture was then stirred overnight and after that, filtered and centrifuged to get the chlorophyll rich extract. It kept at 4^0 C for further use.

3. Lagerstroemia indica (Flower) :

Flowers of Lagerstroemia indica collected, and deionized water used to wash impurities and then dried at 50 ^{0}C in a furnace. The mortar and pestle used to crush dried Lagerstroemia indica flowers into a fine powder. Approximately 2g of Lagerstroemia indica flower powder mixed with 50 ml ethanol, which is stirring overnight at 25 ^{0}C and then kept away from light for 24 h. The solid debris was separated using filtration and centrifugation, and we get the anthocyanin-rich dye solution, it was protected from direct sunlight exposure and stored at 5 °C

.

4. Hollyhocks (*Alcea rosea*):

Flowers of Alcea rosea were taken, cleaned with DI water and then dried in a furnace for 20^0 C temperature. The dried Alcea rosea petals were mashed using mortar and pestle into a granular powder. Alcea rosea powder imbued in ethanol which stirred for 12 h at 25^0 C and then kept away from sunlight for 24 h. The solid debris present in solution was filtered out by filtration, centrifugation, and the dye solution stored at 5^0 C for further use.

Figure3.1 Flower petals of Hollyhocks, Lagerstroemia indica and leafs of Moses rose.

3.1.3 Dye Coating:-

To coat dye on TiO_2 film, we dip the TiO_2 coated FTO substrate into the ethanolic solution of dyes for 24h, and using this dip coating method [27]; Dye gets absorbed on TiO_2 coated FTO. After that, we take out the FTO from the dye solution and then wash it with ethanol to remove unabsorbed dye from FTO.

3.1.4 Electrolyte Preparation:

Dissolve I_2 crystals in a mixture consist of acetonitrile and ethylene glycol now add KI powder into this solution, stir it for 30 minutes, and then setting for 24 hours [28].

3.1.5 Counter Electrode Preparation:

To make counter electrode first wash TCO carefully with the above-given procedure, then coat it with a carbon layer using a candle by holding FTO on the candle flame for 2-3 minutes.

3.1.6 Cleaning of FTO substrates:

FTO coated glasses were used as a substrate for coating. FTO glasses were purchased in 18×18 cm, and then they were cut in a square shape with fixed dimensions 1×1cm. Cleaning was done in following steps

1. FTO glass is ultrasonicated first with acetone for 10 minute and dried it for 5 minute.
2. In second step FTO is ultrasonicated with isopropanol for 10 minute and dried for 5 minute.
3. At last substrate is sonicated with DI water for 10 minute and we kept it in furnace for 10 minute for drying. These FTO substrates were used for the further coating of solar cell materials**.**

3.1.7 TiO_2 Coating:

Oriented Rutile TiO_2 nanorods film was grown on FTO using a simple hydrothermal method in which we placed FTO substrate in the growth solution consists of DI water, HCl, and Titanium butoxide in standing position with conductive side facing the wall of Teflon lined autoclave[29].

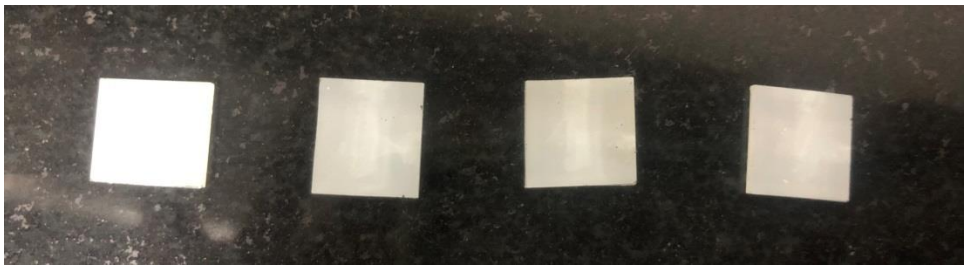

Figure 3.2 Oriented Rutile TiO_2 nanorod films on TCO.

3.1.8 Fabrication of Solar cell:

The arrangement of the DSSC is a sandwich type, and it consists of a photoelectrode coated with a wide bandgap semiconductor which layered with dye, electrolyte, counter electrode with carbon coating on it. After preparing each component of the DSSC successfully, a solar cell was built with the following procedures.

First, we cut FTO glass in 1 × 1 cm dimension and checked for the conductive side. Then we clean FTO using the procedure mentioned above, and we grow TiO_2 nanorods of rutile phase on FTO using a simple hydrothermal method which was only produced on the conductive side.

Now we get our photoelectrode coated with a wide bandgap semiconductor and by using dip coating method to dye to get absorbed onto TiO_2 coated FTO, wash unabsorbed dye with ethanol and our second component is also ready.

To prepare counter electrode first wash FTO carefully with the above-given procedure, then coat it with a carbon layer using a candle by holding FTO on the candle flame for 2-3 minutes.

Now put both electrodes together, using paper binding clips to hold them together, the gap between them is filled with prepared electrolyte, and the device is ready to use.

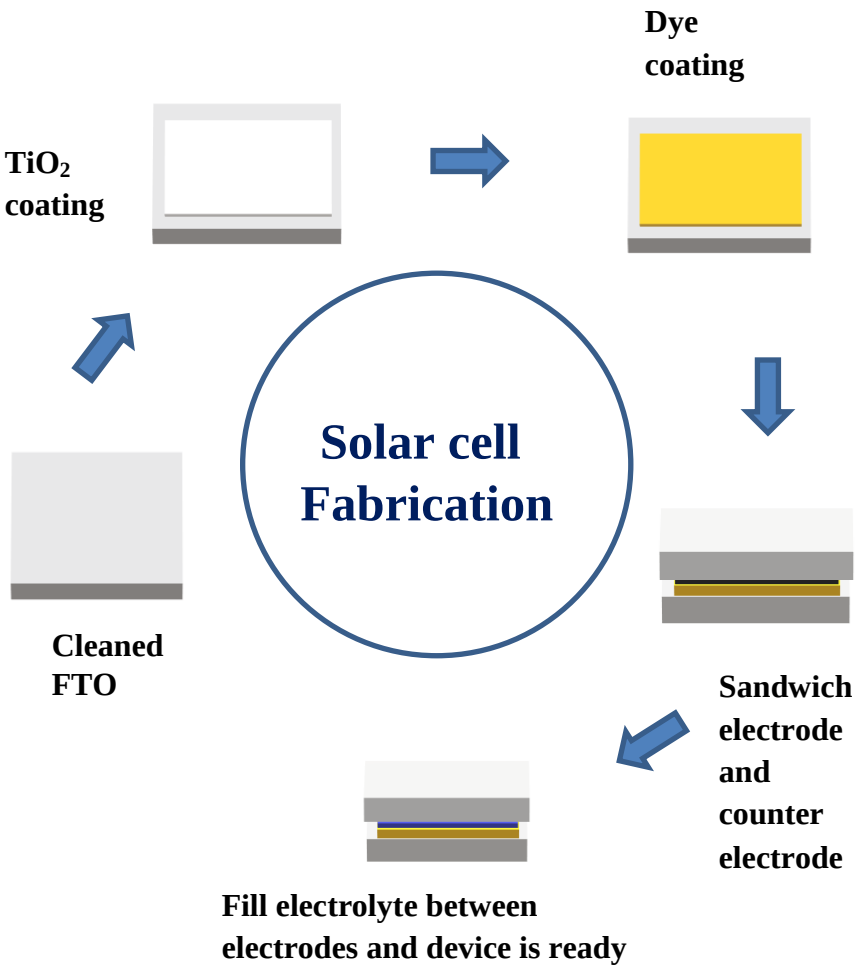

Figure 3.3 Fabrication of Dye Sensitized solar cell

3.2 Characterization Techniques:

3.2.1 XRD:

For the characterization of srystalline material, one of powerful technique that used is X-ray diffraction method, it provides information regarding,

- Lattice and atomic parametres
- Atomic orientation

3.2.1.1 Working principle:

The basic principle of X-ray diffraction method is interferance and diffraction of monochromatic X-ray beams which further scattered at different angles according to the orientation of crystal planes of atoms.The relationship between the X-Ray wavelength (λ), the inter planar distances d_{hkl}, and the angle of the incident beam to planes (θ), is given by the Bragg's law.

$$2d_{hkl} \sin\theta = n\lambda$$

n is the diffraction order

When two seprate waves arrive at a particular point with the same phase. Then there is two possibility of consertive and destructive interference occurs and when it follow bragg's law there will be contructive interface as shown in fig 3.6.

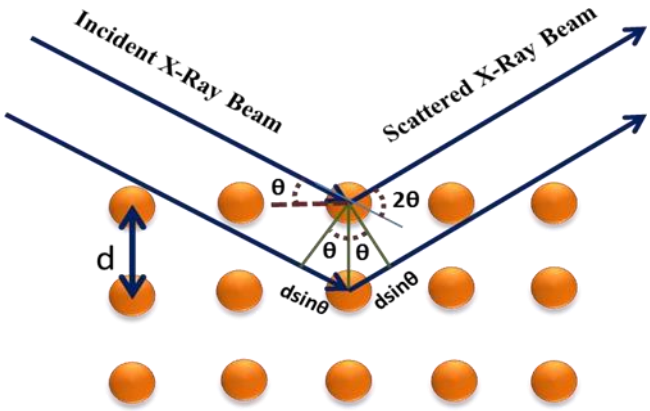

Figure 3.4: Schematic representation of X-Ray diffraction (Bragg's diffraction)

3.2.1.2 Instrumentation:

A powder X-ray diffractometer consists of 3 parts:

- An X-ray source (usually Cu-Kα radiation)
- A sample stage
- A detector

X-rays are formed in a cathode ray tube by heating a filament to generate electrons, quickening the particles toward a specimen by applying a high voltage, and bombarding the target body with electrons. When electrons have enough energy to displace inner shell electrons of the target element, then characteristic X-ray spectra are produced. Cu Kα is generally used as a for the diffraction pattern in XRD having wavelength, λ=1.5418Å. X-rays are incident onto the specimen. The specimen along with the detector, both rotated by an angle of 2 theta and capture all diffracted and reflected X-rays. The whole process fulfills the Braggs law, and the corresponding peak has been occurred with a fixed intensity and at a fixed position. A detector has used to records all signal.

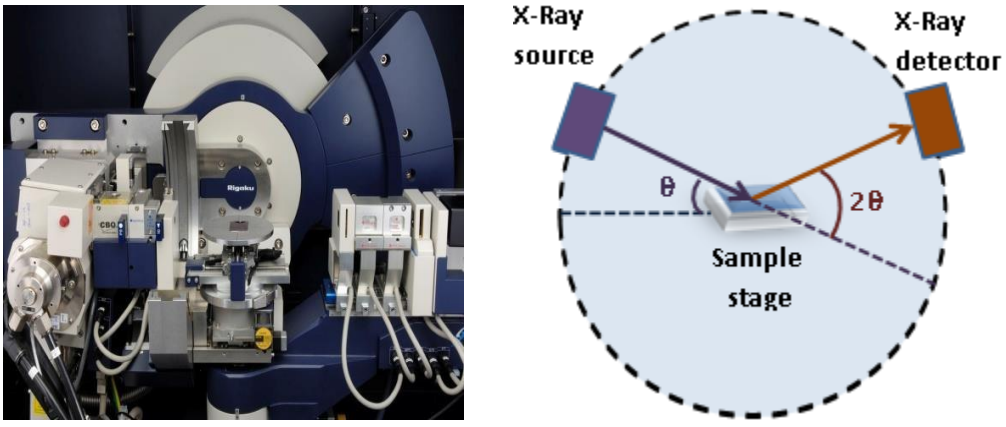

Figure 3.5: (a) X-Ray Diffractometer instrumentation [31].

(b) Schematic representation of instrument.

3.2.2 Scanning Electron Microscope (SEM):

A scanning electron microscope is an advanced model of an electron microscope. SEM is used to study morphology, and we get topographical information about the sample. SEM investigates by a focused electron beam directed over a surface to create an image of the specimen surface. The electrons interact with the specimen and producing various signals collected by a detector which used to obtain information about the surface morphology and topography of the sample.

3.2.2.1 Working principle:

When accelerated prime electrons reachs th surface of the specimen, it generates secondary electrons which further collected by the detector and to produce 3-D picture of the sample

.

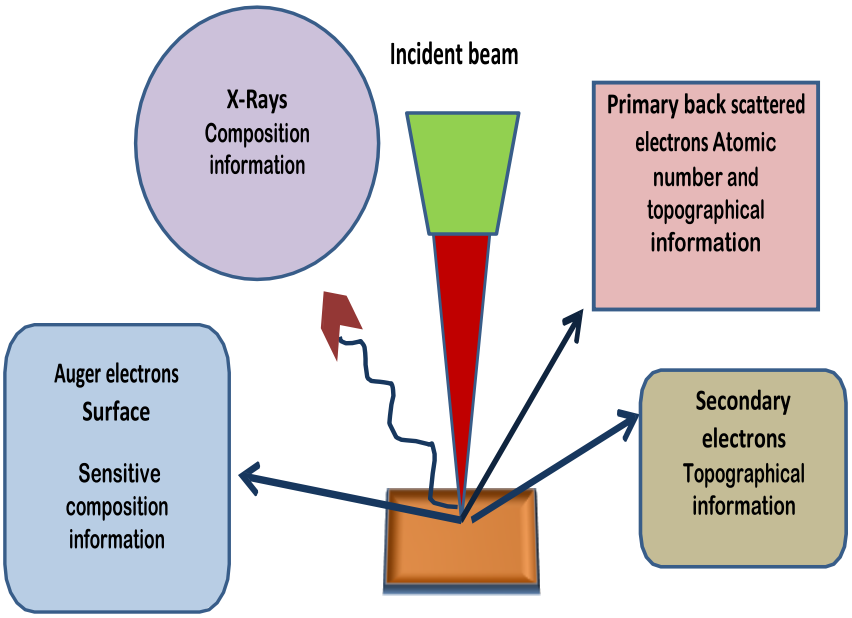

Figure 3.6: Representation of outcomes of incident beam falling on sample in FESEM.

4. **Instrumentation:** At top of the column, the electrons are produced, accelerated down and passed through a succession of lenses and apertures to create a focused beam of electrons, which hits the surface of the specimen, as shown in Fig. 3.5, and 3.6. The specimen is installed on a stage in the chamber region and, the microscope is created to function at low vacuums, a combination of pumps evacuates both the column and the chamber regions. The level of the vacuum in this setup will depend on the configuration of the microscope. Scan coils located above the objective lens, control the position of the electron beam on the sample.

Figure 3.7: Scanning electron microscopy instrumentation .

3.2.3 UV-Vis spectroscopy:

It is a spectroscopy of photons in which we usually study photonic interation in UV-visible region, when ultra violet and visible light is passed through the material , it absorbs some particular amount of wavelength which gives us information about energy bandgap which related to the functional group of material.

3.2.3.1 Basic principle UV spectroscopy obeys the Beer- Lambert's law, which says that: "when a beam of monochromatic light is passed through a solution of an absorbing substance, the rate of decrease of intensity of radiation with thickness of the absorbing solution is proportional to the incident radiation as well as the concentration of the solution."

Beer-Lambert's law express as-

$A = \log (I_0/I) = \varepsilon cl$

Where A is absorbance,

I_0 is intensity of incident light

I (intensity of transmitted light)

C (concentration of solute),

ε is molar absorptivity

l (length path)

3.2.3.2 Instrumentation:

UV-Vis spectrometer consists of monochromatic source of light, specimen, detector for detecting the response, amplifier for the analysis and the recorder.

The light source used for the UV spectrometer is made up of Tungsten filaments and the hydrogen isotope deuterium for the lamp.

This light will pass through a monochromator and further divided into two beams. One divided beam passed through the sample solution, and the second beam passed through the reference solution. Both sample and reference solution contained in the cells made of silica, not glass (glass absorbs light).

Usually in UV spectroscopy has two photocells which are used as detector. One receives the beam from the sample cell, and the other detector collects the beam from the reference. The alternating current produced in the cells carried to the amplifier. Generally, Current delivered in the photocells are of less energy; the principal purpose of an amplifier is to amplify the signals so we can get clear and recordable signals. The computer collects all the data produced and gives the spectrum of the desired compound. The schematics of UV-Vis represented in Figure 3.7.

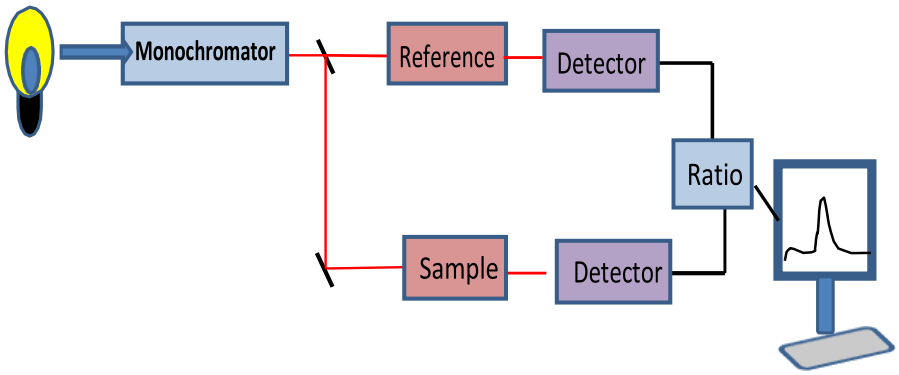

Figure3.8: Diagram of UV visible spectroscopy setup

3.2.3.3 Tauc Plot: *Tauc et al.* suggested a method for determining the band gap using optical absorbance plotted appropriately with energy [45, 46]. They show that the optical absorption strength depends on the difference between the photon energy and the band gap,

as follows

$$\alpha h\nu = B(E_g - h\nu)^m$$

Where α is absorption coefficient, β is an arbitrary constant; E_g is the energy of the optical band gap, and m is the power factor of the transition mode, which depends upon the nature of the material, whether it is crystalline or amorphous.

According to Tauc's relation:

m = 1/2 for direct allowed transitions

m= 3/2 for direct forbidden transitions.

m= 2 for indirect allowed transitions

m= 3 for indirect forbidden transitions

The plots of $(\alpha h\nu)^2$ versus the photon energy ($h\nu$) gives a straight line in a certain space. The extrapolation of this straight line will intercept the ($h\upsilon$)-axis to give the value of the direct optical energy gap (E_g).

CHAPTER 4

RESULT AND DISSCUSION

4.1 Analysis of TiO_2 layer

4.1.1 XRD Analysis of TiO_2 nanorods

The XRD pattern of nanostructured TiO_2 is done to determine phase purity and crystal structure and shown in Fig. 4.1. XRD pattern indicates the formation of tetragonal rutile phase determined from Figure 4.1. All the diffraction peaks of TiO_2 film are in good agreement with the tetragonal rutile phase (SG, P42/mnm; JCPDS No. 04-0551, $a = b$ = 4.5940 nm and c = 2.9580 nm). The deposited film has nanorods which are approximately oriented in perpendicular to the surface of FTO.

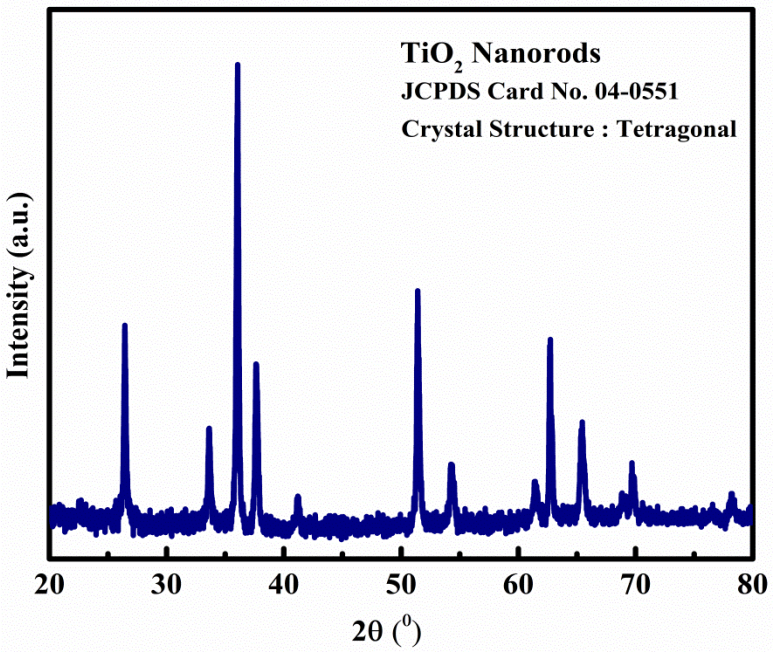

Figure4.1: XRD pattern of TiO_2 Nanorods.

After $TiCl_4$ treatment done on TiO_2 coated FTO, we get the diffraction pattern where (112) plane is missing, and we get the maximum intensity of

(002) peaks as shown in Fig. 4.2. $TiCl_4$ treatment forms a blocking layer of TiO_2 on uncovered area of the TCO, which increase the shunt resistance and enhance the fill factor.

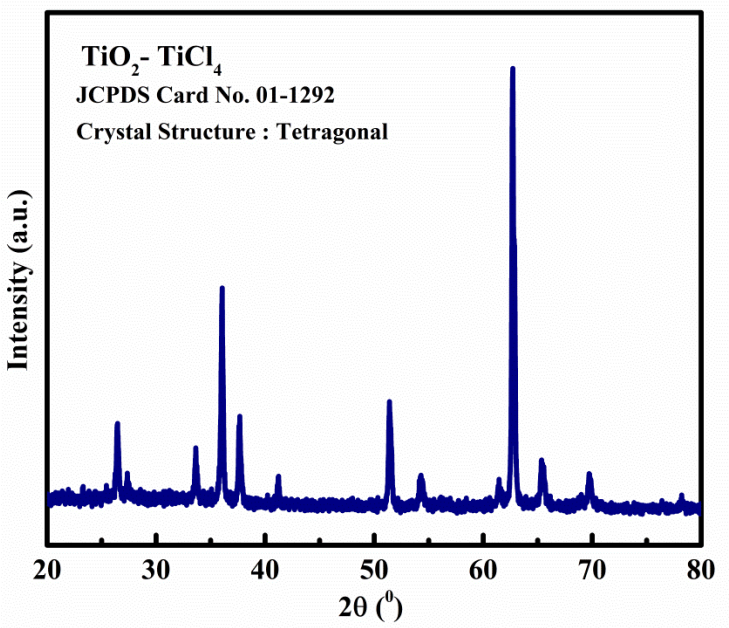

Figure 4.2: XRD pattern of TiO_2-$TiCl_4$ Nanorods.

4.1.2 FESEM analysis TiO_2 Nanorods:

The SEM pictures at distinctive positions and magnifications provide information about nanorod morphology of TiO_2 and uniform growth over entire FTO substrate. Figure 4.3 shows that the top surface of the nanorods look rough with step edges, while on FTO, nanorods grows uniformly.

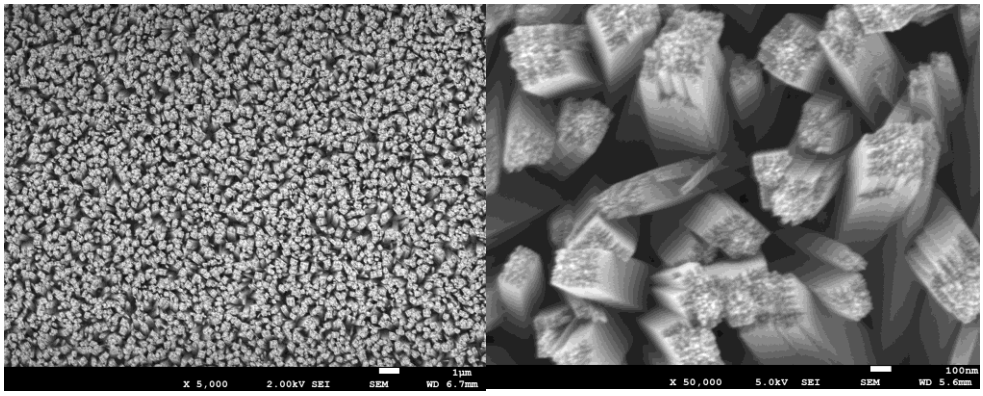

Figure 4.3 SEM images of TiO_2 nanorod film on FTO substrate at different magnification.

In order to get $TiCl_4$ coating TiO_2, we soaked TiO_2 in $TiCl_4$ solution for 45 minutes at 70^0 C, we noted some roughness in FESEM images shown in Figure 4.4

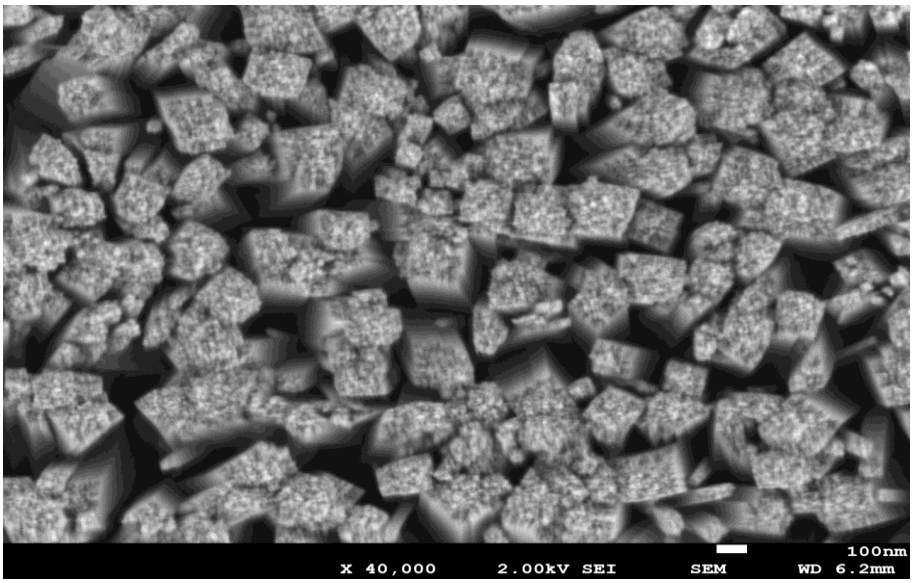

Figure 4.4 FESEM image of $TiCl_4$ coated TiO_2 nanorods.

From the FESEM images, it found that TiO_2 has square top facets on tetragonal rods. The nanorods of TiO_2 are approximately parallel to the normal of FTO surface . After 18 h of synthesis time, the average diameter were 98±5 nm measured using Image J software.

Effect of Growth Time

When the growth time less than 5 hr at 150 ^{0}C, no growth is seen on FTO substrate and it remains transparent. When growth time increased more than 5h, nanorods starts to grow on FTO with nanorod structure but grow with their axis disoriented in all the directions and ultimately collide with neighboring nanorods and growth was stopped. The diameter of nanorods soon reaches around 90 nm and remains same with increase in synthesis time. If the reaction time is increased more than 24 h, a nanorod film starts

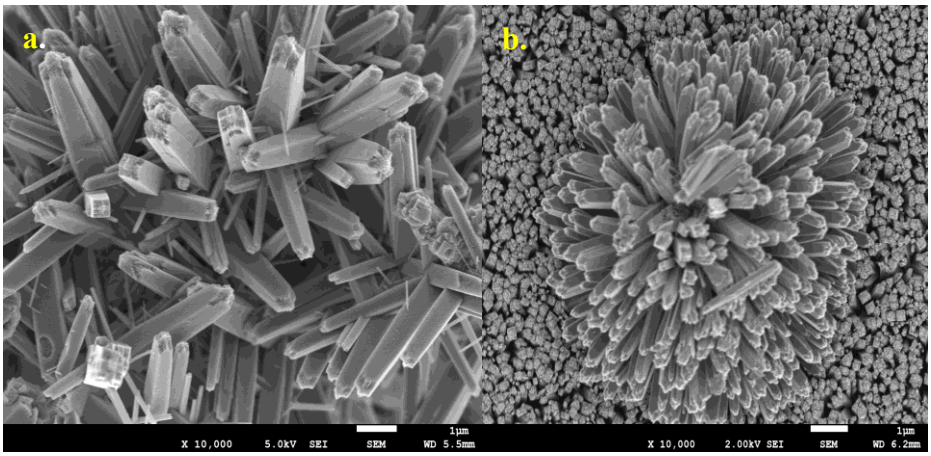

Figure 4.5 FESEM image of TiO_2 nanorods at (a) 10h and (b)14h reaction time.

to peel off the substrate, which is composed of aligned TiO_2 nanorods. The peeling of the white film could be due to a competition between dissolution and crystal [19-21]. When the reaction time is more, the system approaches equilibrium, and the crystal growth rate starts to decrease. TiO_2 nanorods only grow on FTO may be due to matching lattice parameters of FTO and TiO_2 nanorods.

Effect of Growth Temperature

When temperature was less than 100^0 C, TiO_2 nanorods didn't grow on the substrates.

Effect of Substrate

FTO substrates are only one which is suitable for the growth of single directional TiO_2 nanorod film. Attempts to synthesis TiO_2 rods on glass were failed, which means that growth and nucleation may require epitaxy.

Effect of Initial reactant concentration

Nanorods density altered by varing the initial amount of precursor in the growth solution. These FESEM images of TiO_2 nanorod films synthesize at 150^0 C for 18h with a different combination of titanium precursor in growth solution, which is a mixure of 30 ml DI water and 30 ml of HCl.

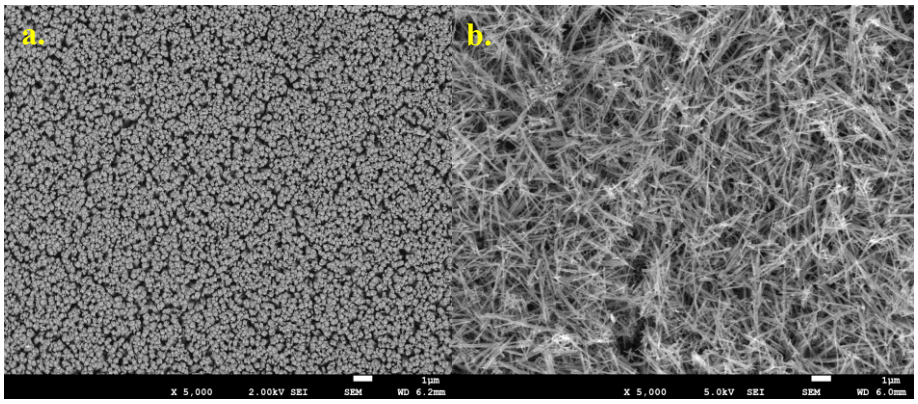

Figure 4.6 FESEM images of TiO_2 nanorods with (a)1 mL and (b)75 mL amount of Titanium butoxide.

4.1.3. UV-Vis spectroscopy

We have done comparative analysis through XRD and FESEM of all the sample and now by UV-Vis spectroscopy, we plot absorption spectra of TiO_2 samples. Absorption spectra have also been analyzed for a thin film after coating. Tauc plot is plotted for TiO_2, and TiO_2-$TiCl_4$. It has excellent absorbing properties (Figure 4.7 and 4.8). They show a direct band gap of 2.8 eV, agrees well with reported data.

4.1.3.1 UV-Vis spectroscopy for TiO_2 thin film:

The optical absorbance was measured by UV–Vis diffuse reflection spectrometer. The photonic absorption for the sample shows the absorption onset of TiO_2 nanorods prepared by hydrothermal method at around 414 nm. The corresponding band gap was calculated as shown in **Fig.4.7 (B)** which is **2.83eV**.

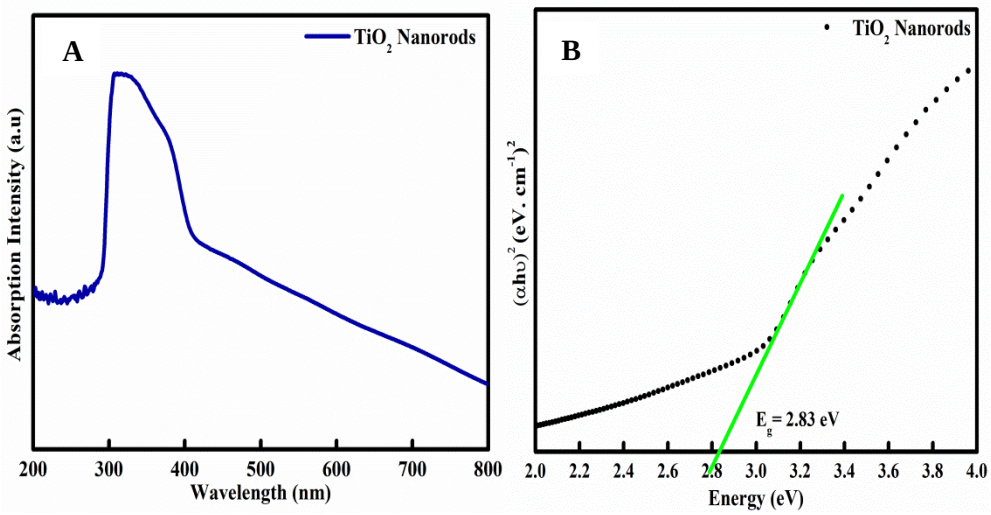

Figure 4.7 UV absorbance and Tauc plot of TiO_2 nanorods.

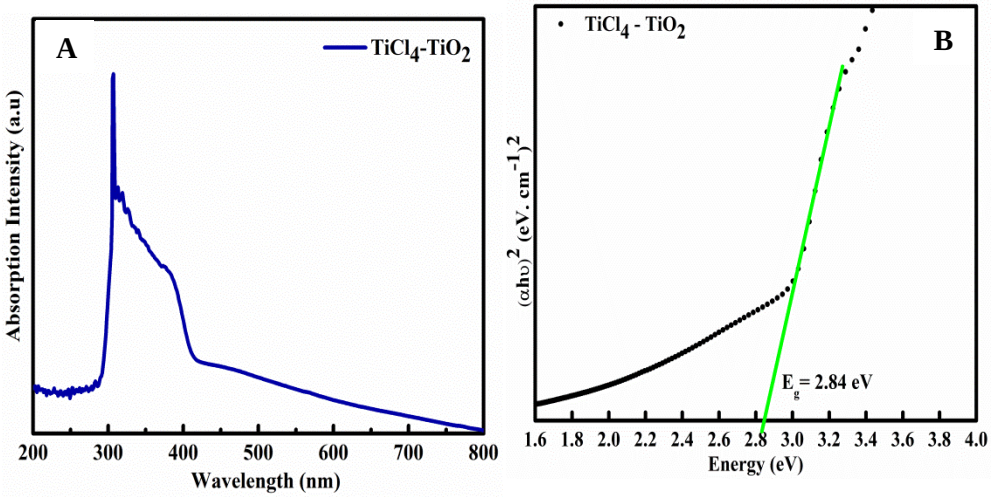

Figure 4.8 UV absorbance and Tauc plot of TiO_2-$TiCl_4$ nanorods.

The absorption onset of TiO_2 nanorods prepared by hydrothermal method is around 421 nm. The corresponding band gap was calculated as shown in **Fig. 4.8 (B)** by Tauc plot and which is **2.84 eV**.

4.1.4. Raman spectroscopy analysis

The rutile TiO_2 has tetragonal phase and shows symmetry characteristics of the space group with two TiO_2 molecules and eight atom per unit cell. Four Raman active modes were found A_{1g}, B_{1g}, $B_{2g,}$ and E_g in the rutile TiO_2 single crystal at 142 (B_{1g}), 445 (E_g), 608 (A_{1g}), and 237 (B_{2g}) cm^{-1} expressed as Rutile = A_{1g} + B_{1g} + B_{2g} + E_g. Among these peaks, the two raised maxima at 445 (E_g) and 608 cm^{-1} (A_{1g}), are in well agreement with reported for the rutile phase TiO_2 crystal. The Raman peak at 237 cm^{-1} is due to the multiple-phonon scattering processes, which a characteristic Raman peak of rutile type TiO_2 [32].

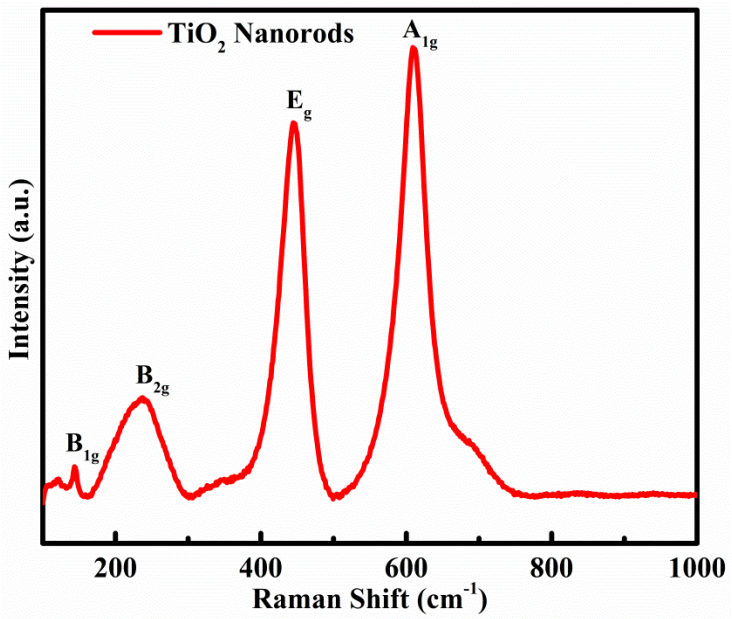

Figure 4.9 Raman Spectroscopy of TiO_2 nanorods.

4.2. Analysis of Dyes

The absorption of dye with wide absorption spectrum on the TiO_2 with anchoring groups present as carboxylic(COOH), carbonyl(CO), and

hydroxyl(OH) [33]. Good adsorption of the dye onto the nanostructured semiconductor is expected for the efficient electron transfer into the conduction band of the wide band gap semiconductor which is here TiO_2. So, UV-Vis spectroscopy of all dyes is done to analyze absorption spectra.

4.2.1 UV- Vis Absorption Spectra

The absorption spectra of all four dyes is shown in **Figure 4.10.**

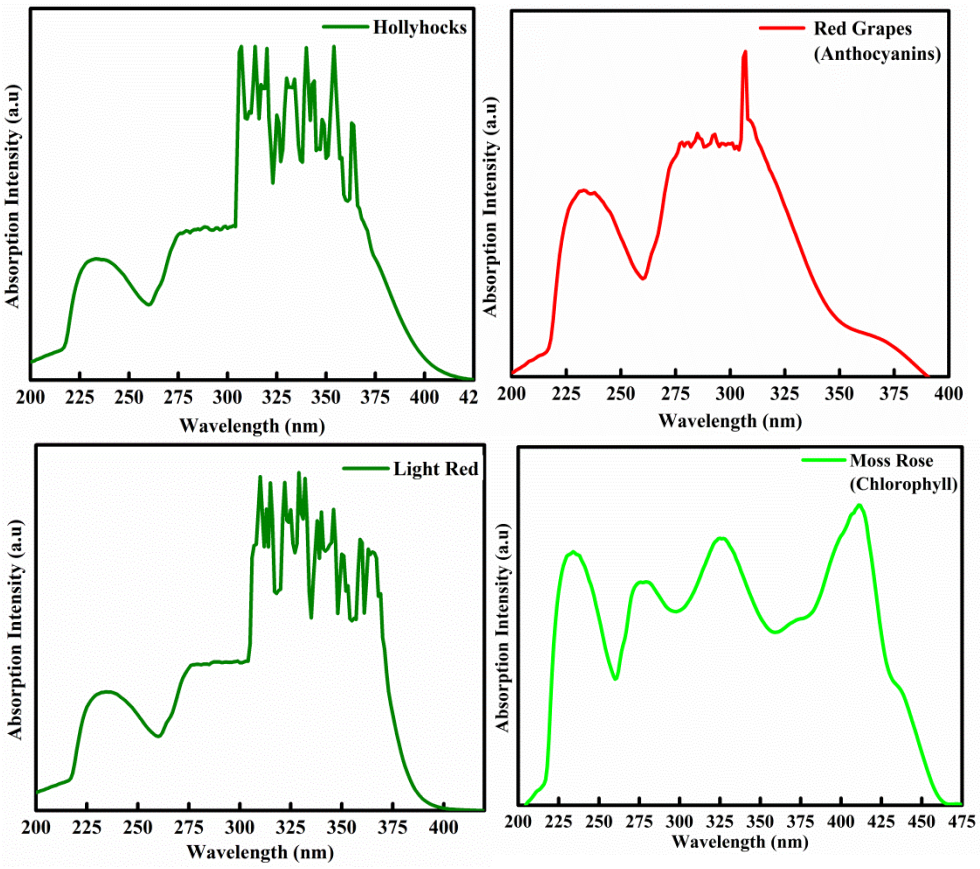

Fig. 4.10 shows absorption spectra for (*a*) Moses rose, (*b*) hollyhocks, (*c*) red graps and (*d*) Lagerstroemia indica

The absorption onsets of Moss rose, Hollyhocks, Red grapes and Lagerstroemia indica are 460, 425, 390 and 400 nm, respectively The

absorption onsets of Moss rose, Hollyhocks, Red grapes and Lagerstroemia indica are 460, 425, 390 and 400 nm, respectively.

4.3. I-V measurement:

Efficiency for solar cell (PCE) is denoted by ɳ calculated by using the following formula,

$$\text{Ɔ} = \frac{V_{oc} I_{sc} FF}{P_{in}}$$

V_{oc} is the open-circuit voltage,

I_{sc} is the short-circuit current,

FF is the fill factor, where $FF = \frac{V_{max} I_{max}}{V_{oc} I_{sc}}$

Ɔ is the efficiency

I-V measurements have been carried out by solar simulator (Photo Emission Tech., Inc., Model-SS50AAA-EM) for DSSC with all four dyes.

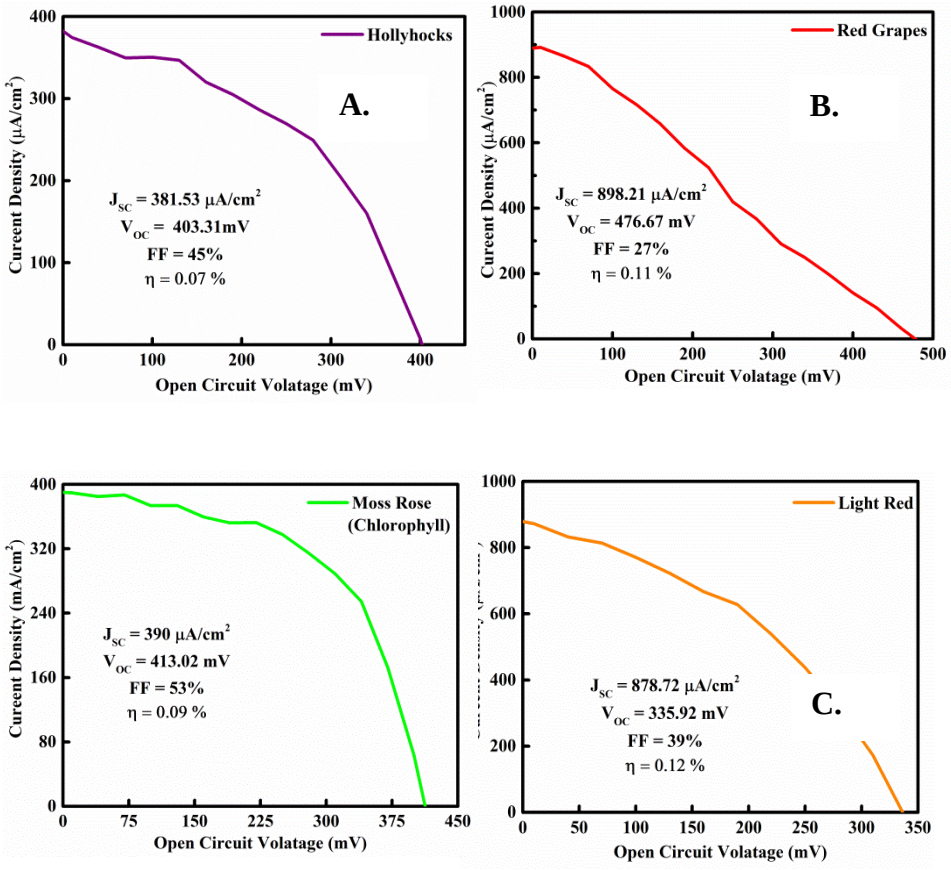

Figure 4.11 I-V measurement for dyes (a) Hollyhocks, (b) Red Grapes (c) Moss Rose and (d) Lagerstroemia indica

Figure 4.11 shows *I-V* measurement for all four dyes. Highest efficiency has been achieved for Lagerstroemia indica η =0.12%. While for Red Grapes it is 0.11%, for Moss Rose efficiency is 0.09% and for Hollyhocks, it is 0.07%.

4.4 Comperative table of natural dyes

Table 4.1 Efficincy of natural dyes in DSSC.

Dye	**Semiconductor oxide**	**J_{sc} ($\mu A/cm^2$)**	**V_{oc} (mV)**	**FF**	**ŋ (%)**
Rose	TiO_2	970	590	65	0.30 [33]
Dragon Fruit	TiO_2	200	220	30	0.22 [33]
Shiso	TiO_2	356	550	51	1.01 [33]
Moses Rose	TiO_2	390	413.02	53	0.09 (This report)
Holy hocks	TiO_2	381.53	403.31	45	0.07 (This report)
Red grapes	TiO_2	899.21	476.67	27	0.11 (This report)
Lagerstroemia indica	TiO_2	878.72	335.92	39	0.12 (This report)

In the above table, we compared different reported natural dyes with efficiency. Our reported values are seems to be comparable with earlier reported data however these can be improved further . As present we didn't use Pt and conducting carbon for electrode fabrication, implementation of these will provide much more higher efficiency. In future it is planned to concentrate on these.

CHAPTER 5

CONCLUSIONs AND FUTURE SCOPE

5.1 Conclusions:

Here in this theis, we have synthesized rutile TiO_2 nanorods film (with different parameter), four dyes and electrolyte for our DSSC device fabrication. We used a hydrothermal reaction to synthesis rutile TiO_2 nanorods. After synthesis, we have characterized rutile TiO_2 nanorods to study the structural, morphological, and optical property. For structural property, XRD pattern has been analyzed for all TiO_2 films with different parameters. A comparative analysis has been done among all films.

Interestingly we got a quite dense nanorods film grown at 180^0 C for 18h with 30mL DI water, 30mL HCL and Titanium butoxide. For morphological property, we have done FESEM analysis for all TiO_2 films that show the formation of tetragonal structures highly oriented rods along FTO surface. UV-Vis spectroscopy was done for TiO_2 film and dyes. The optical characterization confirms the strong visible absorption of TiO_2 with an optical bandgap of 2.78-2.8 eV. Finally, attempts have been made to fabricate a photovoltaic device using all four dyes, TiO_2 film, and electrolyte. We have calculated efficiency for Lagerstroemia indica and found η =0.12%. While for Red Grapes it is 0.11%, for Moss Rose efficiency is 0.09%, and for Hollyhocks, it is 0.07%. Dyes are tested for the first time for applications in DSSC. It is safely concluded that Lagerstroemia indica is the best dye among all four dyes.

5.2 Future Scope:

To deliver commercial applications of these DSSCs, it's crucial to reach comparable optical and photovoltaic performance by reengineering TiO_2 with natural dyes which are one of the deliverables of this project. Till date, the PCE of the natural dye-based solar cell is low. Therefore, our intense effort is to optimization all the elements of Dye-Sensitized solar cell with the intent to build more efficient and durable cells with natural dyes.

REFERENCES

[1] Century, R.E.P.N.f.t.s., Renewable's Global Status Report: Update 2009. 2009.

[2] BP, BP Statistical Review of World Energy. 2010.

[3] Agency, I.E., Trends in Photovoltaic Applications: Survey report of selected IEA countries between 1992 and 2008. Photovoltaic Power Systems Programme, 2009.

[4] Solomon, S., Climate change 2007-the physical science basis: Working group I contribution to the fourth assessment report of the IPCC. Cambridge University Press, 4. 2007

[5] Umwelt, B.f., Erneuerbare Energie in Zahlen: Nationale und internationale Entwicklung Berlin. Naturschutz und Reaktorsicherheit, 2009.

[6] Oregan, B. and M. Gratzel, A Low-Cost, High-Efficiency Solar-Cell Based on Dye-Sensitized Colloidal TiO2 Films. Nature, 353(6346): p. 737-740. 1991.

[7] Ito, S., et al., Fabrication of thin film dye sensitized solar cells with solar to electric power conversion efficiency over 10%. Thin Solid Films, 516(14): p. 4613-4619. 2008

[8] Bisquert, J., et al., Physical chemical principles of photovoltaic conversion with nanoparticulate, mesoporous dye-sensitized solar cells. Journal of Physical Chemistry B, 108(24): p. 8106-8118. 2004.

[9] Wang, P., et al., High efficiency dye-sensitized nanocrystalline solar cells based on ionic liquid polymer gel electrolyte. Chemical Communications, (24): p. 2972-2973. 2002.

[10] Snaith, H.J., et al., Efficiency enhancements in solid-state hybrid solar cells via reduced charge recombination and increased light capture. Nano Letters,. 7(11): p. 3372-3376. 2007.

[11] Gao, F., et al., Enhance the optical absorptivity of nanocrystalline TiO2 film with high molar extinction coefficient ruthenium sensitizers for high performance dye-sensitized solar cells. Journal of the American Chemical Society, 130(32): p. 10720-10728. 2008.

[12] Becquerel, E., Recherche sur les e est de la radiation chimique de la lumi ere solaire, au moyen des courants electriques. Comptes rendus hebdomadaires des s eances de l'Acad emie des Sciences, (9): p. 4. 1839.

[13] Cohen, I.B. and A. Einstein, An Interview with Einstein. Scientific American, 193(1): p. 69-73. 1955.

[14] Planck M., Ueber das Gesetz der Energieverteilung im Normalspectrum. Annalen der Physik,. 4: p. 10. 1901

[15] Luque, A., Handbook of Photovoltaic Science and Engineering. John Wiley & Sons, 2003.

. Wurfel, P., Weinheim 2nd edition Wiley-Vch, 2009.

[16] Wenger, S., Strategies to Optimizing Dye-Sensitized Solar Cells: Organic Sensitizers, Tandem Device Structures, and Numerical Device Modeling. PhD thesis École Polytechnique Federale De Lausanne, 2010.

[17] Shockley, W. and H.J. Queisser, Detailed Balance Limit of Efficiency of P-N Junction Solar Cells. Journal of Applied Physics, 32(3): p. 510.1961.

[18] NREL. Best research-cell efficiencies, August 2014.

[19] N. K. Noel.; S. D. Samuel.; A. Abate.; C. Wehrenfennig.; S. Guarnera.; A. Haghighirad.; A. Sadhanala.; G. E. Eperon.; S. K. Pathak.; M. B. Johnston.; A. Petrozza.; L. M. Herza.; H. J. Snaith. Lead-free organic-inorganic tin halide perovskites for photovoltaic applications. Energy and Environmental Science, 7:3061–3068, 2014.

[20] H. J. Queisser W. Shockley. Detailed balance limit of efficiency of pn junction solar cells. Journal of Applied Physics, 32(3):510–519, 1961.

[21] Singh, G. K. (2013). Solar power generation by PV (photovoltaic) technology: A review. Energy, 53, 1-13.

[22] Yoo, K., Kim, J. Y., Lee, J. A., Kim, J. S., Lee, D. K., Kim, K., ... & Kim, J. H. (2015). Completely transparent conducting oxide-free and flexible dye-sensitized solar cells fabricated on plastic substrates. ACS nano, 9(4), 3760-3771.

[23] O'regan, B., & Grätzel, M. (1991). A low-cost, high-efficiency solar cell based on dye-sensitized colloidal TiO2 films. nature, 353(6346), 737.

[24] Narayan, M. R. (2012). Dye sensitized solar cells based on natural photosensitizers. Renewable and Sustainable Energy Reviews, 16(1), 208-215.

[25] Hug, H., Bader, M., Mair, P., & Glatzel, T. (2014). Biophotovoltaics: natural pigments in dye-sensitized solar cells. Applied Energy, 115, 216-225.

[26] Ludin, N. A., Mahmoud, A. A. A., Mohamad, A. B., Kadhum, A. A. H., Sopian, K., & Karim, N. S. A. (2014). Review on the development of natural dye photosensitizer for dye-sensitized solar cells. Renewable and Sustainable Energy Reviews, 31, 386-396.

[27] Mathew, S., Yella, A., Gao, P., Humphry-Baker, R., Curchod, B. F., Ashari-Astani, N., ... & Grätzel, M. (2014). Dye-sensitized solar cells with 13% efficiency achieved through the molecular engineering of porphyrin sensitizers. Nature chemistry, 6(3), 242.

[28] Noda, Y., Kaneyuki, T., Mori, A., & Packer, L. (2002). Antioxidant activities of pomegranate fruit extract and its anthocyanidins: delphinidin,

cyanidin, and pelargonidin. Journal of agricultural and food chemistry, 50(1), 166-171.

[29] Hou, D. X., Fujii, M., Terahara, N., & Yoshimoto, M. (2004). Molecular mechanisms behind the chemopreventive effects of anthocyanidins. BioMed Research International, 2004(5), 321-325.

[30] Su, C., Hong, B. Y., & Tseng, C. M. (2004). Sol–gel preparation and photocatalysis of titanium dioxide. Catalysis Today, 96(3), 119-126.

[31] Liu, Bin, and Eray S. Aydil. "Growth of oriented single-crystalline rutile TiO2 nanorods on transparent conducting substrates for dye-sensitized solar cells." Journal of the American Chemical Society 131.11 (2009): 3985-3990.

[32] Ohsaka, Toshiaki, Fujio Izumi, and Yoshinori Fujiki. "Raman spectrum of anatase, TiO2." Journal of Raman spectroscopy 7.6 (1978): 321-324.

[33] Ghann, William, et al. "Fabrication, optimization and characterization of natural dye sensitized solar cell." Scientific reports 7 (2017): 41470.